IEEE International Conference on Space Optical Systems and Applications,
Vancouver, Canada, 11–13 October 2023

# Prototype test results of a High-Altitude Pseudo-Satellite laser communication terminal

Remco den Breeje,
Arno De Lange, Jorne Boterman,
Martijn Visser, Lex Meijer
*Airbus Netherlands*
*Leiden, The Netherlands*
r.den.breeje@airbusds.nl

Martijn Stopel, Ioannis Proimadis
*VDL ETG*
*Eindhoven, The Netherlands*

Harry de Man
*TNO*
*Delft, The Netherlands*

***Abstract*—High-Altitude Pseudo-Satellites (HAPS) platforms offer a cost-effective solution for remote connectivity with uninterrupted 24/7 availability, presenting a compelling alternative to conventional orbiting satellites. Integrating laser communication terminals onto HAPS platforms enhances their capabilities, enabling high bandwidth and long-distance remote connectivity. In this context, we present Skyline S2, a laser communication terminal for the Zephyr High-Altitude Pseudo-Satellite, a solar-powered platform developed by Airbus, operating in the stratosphere.**

**The Skyline S2 Laser Communication Terminal (LCT), a collaborative development effort between Airbus Netherlands and partners, will enable a 1 Gbit/s inter-Zephyr bi-directional link, spanning distances of up to 100 km. We have designed a novel compact 40 mm aperture LCT that meets the stringent requirements concerning mass, size, and power consumption, while being capable of withstanding the harsh environmental conditions of ambient temperature and air pressure.**

**This paper focuses on the early stages of development, during which prototype lab tests were conducted to mitigate potential risks. The fine steering mirror control performance, the resulting fibre coupling efficiency, and 1 Gbit/s free space communications link test results are discussed. Additionally, this paper summarizes the Skyline S2 design and outlines our roadmap for future developments and Zephyr flight experiments.**

***Index Terms*—Laser Communication, High-Altitude Pseudo-Satellites, stratosphere**

## I. Introduction

### A. HAPS Connectivity

The ever-growing demand for data has led to an increasing need for non-terrestrial networks. These networks offer extensive coverage and resilience, making them a valuable complement to ground-based networks. Non-terrestrial networks consist of a combination of geostationary (GEO) satellites, low-earth orbit (LEO) satellites, and High-Altitude Platform Systems (HAPS). These interconnected platforms, visualised in Fig. 1, operate beyond the limitations of terrestrial infrastructure and play a crucial role in enhancing broadband telecommunications and disaster management.

While GEO satellites have served as the telecommunication backbone for several decades, the rapid deployment of LEO

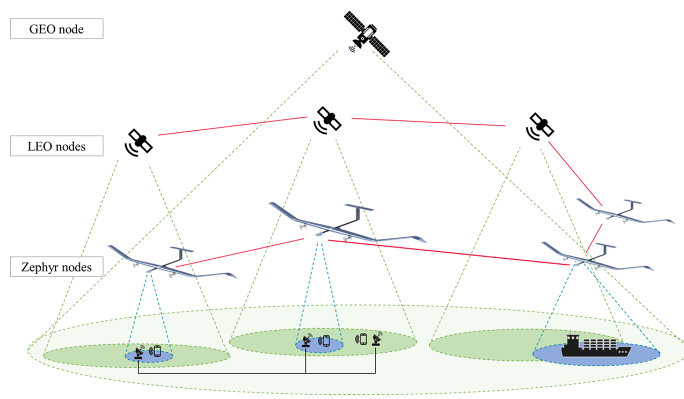


Fig. 1. Multi-layered network of inter-connected GEO, LEO, and HAPS nodes

constellations has been a recent development. Another exciting addition to connectivity platforms is HAPS, bringing greater coverage flexibility and scalability. This flexibility allows for on-demand coverage in remote or disaster-stricken areas where terrestrial infrastructure is lacking or disrupted. Additionally, HAPS platforms have the advantage of a short link distance compared to LEO and GEO nodes, enabling high-bandwidth and direct-to-device RF links. They can provide 24/7 availability by continuously covering specific areas.

Airbus AALTO is deploying connectivity services as part of a future wireless connectivity ecosystem using the Zephyr fixed-wing, solar-powered HAPS platform.

### B. Inter-HAPS Optical Communication Links

Optical links can play an important role in HAPS applications by interconnecting AALTO's Zephyrs and satellite nodes, and offering secure high-bandwidth user links. The primary application currently under development is the inter-Zephyr laser communications link, enabling Q-band RF feeders for remote 5G/6G connectivity hubs as reported in [1]. For this use case, both Zephyr platforms are equipped with a Laser Communication Terminal (LCT) for a high-bandwidth optical communications link. This link relays data from on-board Q-band terminals with on-ground RF antennas to feed the HAPS. See Fig. 2 for the envisioned flight experiment configuration.

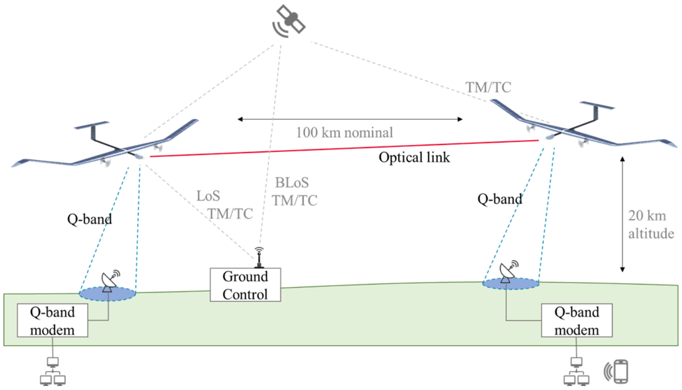


Fig. 2. Flight experiment configuration of the AALTO Zephyr with Q-band feeder and optical inter-HAPS link

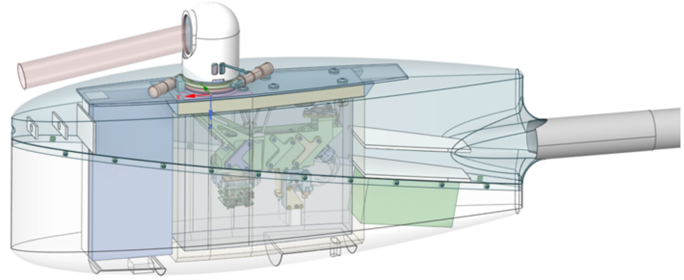

Fig. 3. Skyline S2 LCT in nose-pod configuration

The Q-band terminals can provide a capacity of up to 1 Gbit/s full-duplex. User-data is modulated on-ground, and processed by an on-board RF modem. The data is re-modulated onto the optical carrier to transfer the data to the counter-terminal at a nominal distance of 100 km. The on-board optical modem on the counter-terminal then processes the data for re-transmission to ground through the RF link. This regenerative communication architecture is considered the most robust architecture for this current use case. For higher throughput, an analogue transparent communication architecture can be implemented with minor modifications to the LCT design.

### C. Technical Challenges

A number of technical challenges arise from this inter-Zephyr LCT use case:

*1) Pointing and acquisition:* Laser communication links offer higher throughput over long distances compared to RF, but they require more complex pointing, acquisition, and tracking (PAT) mechanisms. A low-bandwidth telemetry and command (TM/TC) link that is used to configure the Zephyr network will be used to share the GPS location of the counter-Zephyr, enabling the acquisition of the laser link.

The primary source of pointing uncertainty arises from the orientation of the Zephyr. To address this, a low-size and low-weight dual antenna GNSS-Aided Inertial Navigation System (INS) is utilized to determine the attitude of the LCT before link acquisition. The flight-proven acquisition scheme from the Airbus European Data Relay System (EDRS) [2], as also applied in the SDA Optical Inter-satellite Links, is adopted to ensure robust PAT.

*2) Stratospheric environment:* The lower stratosphere temperature typically ranges between -40°C and -80°C, which poses a challenge of finding a balance between thermally isolating the LCT for the night-time scenario and avoiding overheating of the active components during daytime. The daytime solar irradiation on the Zephyr LCT pod in combination with low air pressure makes the -40°C daytime temperature a challenging condition, with overheating as a risk. The thermal design of the Zephyr LCT supports this wide range of environmental conditions by applying a balanced combination of thermal isolation and heater circuits.

*3) Stratospheric beam propagation:* The atmospheric turbulence conditions at low air pressure in the stratosphere are expected to be relatively mild. The atmospheric turbulence will affect the propagation of the laser beam, resulting in intensity fluctuations (on-axis scintillation) and pointing errors (beam wander). When taking the Hufnagel-Valley 5/7 model, the on-axis scintillation index ${\sigma_I}^2$ according to Andrews in [3] is at most 0.11. Following the weak-turbulence scintillation fading-loss threshold strategy of [4], this results in a recommended link budget margin of -3.8 dB to ensure a fade probability threshold of 1%. The influence of untracked beam wander due to turbulence is expected to be negligible.

*4) Size, weight, and power:* Lastly, the HAPS platform imposes stringent requirements on size, weight, and power. The complete LCT design weighs approximately 3 kg and consumes between 30 and 40 Watt of electrical power, depending on the requested transmit laser power.

## II. HAPS Laser Communication Terminal design

The Zephyr LCT, shown in Fig. 3, features a 40 mm diameter aperture, enabling a bi-directional link initially capable of data transmission at 1 Gbit/s with a range of 100 km. The 40 mm aperture LCT design allows for future upgrades to higher bandwidths and longer distances, maintaining a high link budget margin during the initial demonstration phase.

The Zephyr LCT comprises several key subsystems: an Optical Bench, a Coarse Pointing Assembly (CPA), an Optics Control Unit, a Laser Module and an Optical Modem. The LCT interfaces with the on-board RF modem and Zephyr Controller, residing in the nose pod of the Zephyr. The interconnects between the various subsystems are shown in Fig. 4.

*1) Optical Modem:* The Optical Modem is responsible for real-time coding and decoding of the 1 Gbit/s full-duplex data stream. It employs bit and frame markers, as well as Reed–Solomon coding and interleaving, to synchronize the data streams and correct errors.

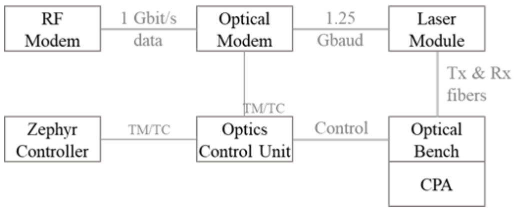


Fig. 4. HAPS LCT block diagram

*2) Laser Module:* The Laser Module houses the amplifier stages, seed laser, external modulator, and optical detector, which are interfaced by the Optical Modem. The custom-designed Laser Module by G&H [5] provides a 1.2 Watt transmit laser signal (average, post-modulation) via a compact 2-stage amplifier, and pre-amplifies the received laser signal before detection, enhancing the optical signal-to-noise ratio. The transmit laser power can be adjusted based on the link conditions to prevent saturation at the receiving terminal, while simultaneously optimizing electrical power consumption.

*3) Optics Control Unit:* The Optics Control Unit, based on a System-on-Chip FPGA and ARM CPU combination, manages real-time control of the Optical Bench and CPA, and implements on-board embedded software for autonomous operation. It also handles external telemetry and telecommand functions and locally controls the Laser Module and Optical Modem.

*4) Nose pod:* The LCT will be integrated into the Zephyr's aerodynamic nose pod configuration, with the CPA protruding from the top to ensure free horizontal line of sight while safeguarding delicate optics and mechanics during landing.

*5) Optical architecture:* The optical architecture, as depicted in Fig. 5, employs a mono-static design with a 40 mm aperture, collimating a single-mode fibre transmit signal and injecting the received signal into the single-mode receive fibre. A portion of the received light is allocated for the Acquisition and Tracking Sensor (ATS), facilitating wide-field view during acquisition (± 0.9°) and high-bandwidth control tracking once the optical link is established. A Fine Steering Mirror (FSM) scans the uncertainty cone during acquisition and corrects system pointing errors during tracking to ensure precise alignment with the counter-terminal and efficient coupling into the receive fibre.

The CPA offers continuous 360° azimuth rotation and ±8° elevation-axis pointing, designed for horizontal inter-Zephyr links. The CPA tracks the counter-terminal, compensates for Zephyr attitude variations, and offloads DC components of the FSM control loop.

### A. Link Budget

A large-margin link budget is defined in Table I, allowing for future enhancements in data throughput capacity and link distance. The receiver optical loss accounts for splitting loss towards the ATS and fibre coupling efficiency. Though pointing errors dominate single-mode fibre coupling loss, the optical pre-amplifier compensates for this. The use of single-mode fibre allows for potential upgrades to high-throughput (coherent) transceivers in the future.

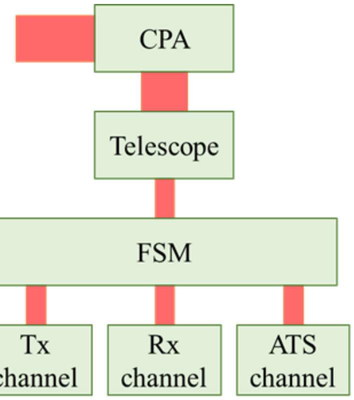


Fig. 5. Skyline S2 LCT optical architecture

TABLE I
LCT OPTICAL LINK BUDGET

| | | |
|---|---|---|
| **Tx Power** | | |
| Tx power | dBm | 30.8 |
| **Tx Antenna** | | |
| Tx wavelength | nm | 1550 |
| Antenna gain | dB | 91.2 |
| Transmission loss | dB | -1.0 |
| Pointing loss | dB | -3.0 |
| **Free Space** | | |
| Slant range | km | 100 |
| Propagation loss | dB | -238.2 |
| Atmospheric attenuation loss | dB | -3.0 |
| Atmospheric scintillation margin | dB | -3.8 |
| **Rx Antenna** | | |
| Rx telescope diameter | mm | 40 |
| Antenna gain | dB | 98.2 |
| Transmission loss | dB | -1.0 |
| **Rx Optical Path** | | |
| Receiver optical loss | dB | -7.5 |
| Effective irradiance | dBm | -37.3 |
| Required irradiance with FEC | dBm | -47.5 |
| Margin with FEC | dB | 10.2 |

In the following section, we discuss the forward error correction (FEC) technique, which significantly improves link efficiency by more than 5 dB while introducing a coding overhead of less than 7%. The link can also operate without FEC, in which case the link budget margin remains at 4.8 dB.

## III. EARLY PROTOTYPE TEST RESULTS

As part of the Zephyr LCT flight prototype design process, early prototype tests are being conducted to verify the system's performance. The Early Prototype setup comprises two optical benches operating in controlled laboratory conditions. The optical bench design mirrors the optical architecture of the flight prototype, encompassing essential components such as a reflection-based telescope, the Fine Steering Mirror (FSM)

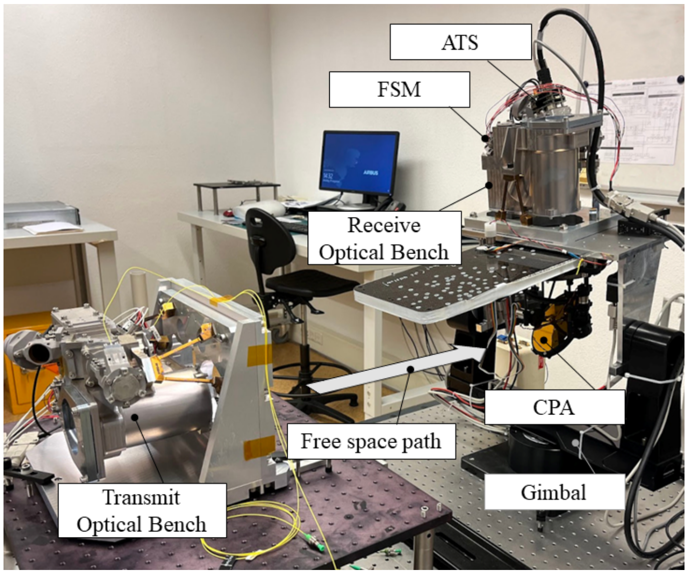


Fig. 6. HAPS LCT Early Prototype setup

actuator, a camera-based Acquisition and Tracking Sensor (ATS), and single-mode fibre coupling.

In this setup, shown in Fig. 6, one optical bench is equipped with a Coarse Pointing Assembly (CPA) and is mounted on a gimbal system that replicates the movements and orientations expected during Zephyr's flight. This emulation of Zephyr's movements allows for assessing the performance of the LCT in dynamic scenarios. The other optical bench remains in a static configuration.

We report the test results of the following key tests that have been conducted with the Early Prototype setup:

- Fine Steering Mirror control loop
- Fibre Coupling Efficiency
- 1 Gbit/s Communications Link

### A. *Fine Steering Mirror control loop*

In order to successfully maintain precise alignment of the LCTs during acquisition, the dynamic positioning error must be kept below 10 µrad. This defines a challenging requirement as the LCT is subject to various disturbance sources, including aerodynamic and Zephyr propellers-induced vibrations, as well as errors induced by the motion of the host and remote Zephyrs. To satisfy such a requirement, the control architecture relies on both the CPA and FSM positioning mechanisms, which are capable of performing tip/tilt rotations, while the resulting displacement of the incoming beam (in case of a receive mode) is measured by the ATS. The control architecture is implemented on the FPGA and the closed loop system runs at 5 kHz sampling frequency. The control architecture is shown in Fig. 7.

By employing the difference between measured and reference ATS spot location, where the reference location corresponds with the maximum fibre coupling position, the FSM feedback controller computes the required FSM correction command. The FSM actuator is designed in such a way that it exhibits an almost linear behavior along its operating range [6], [7]. The frequency response of the FSM actuator to the resulting ATS position is determined in system-identification tests, and is used to design a high (>250 Hz) bandwidth linear controller as shown in Fig. 8.

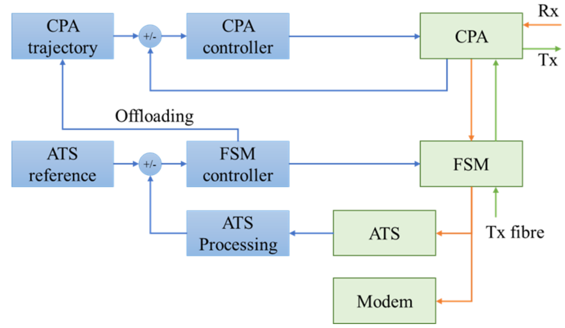


Fig. 7. Simplified control architecture (left) and hardware structure (right)

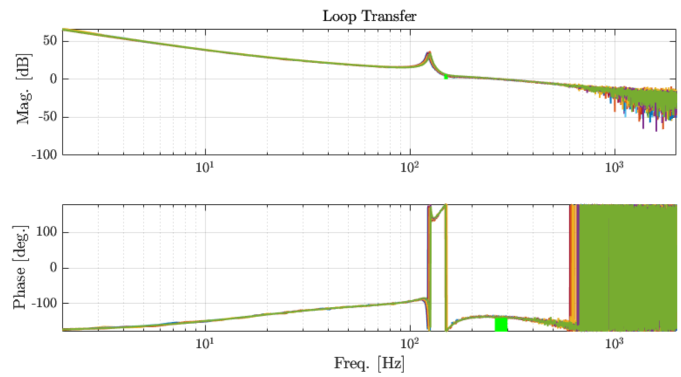


Fig. 8. Frequency response of the FSM loop transfer (FSM error to ATS spot) around the $x$ axis at different operating points (similar results were obtained for the $y$ axis). The resulting bandwidth for all the investigated FSM angular offset positions is above 250 Hz.

The FSM and CPA controllers work in synergy. The CPA predominantly compensates the large positioning errors in a coarse manner, while the FSM takes over the fine, µrad-accurate positioning corrections. In order to ensure that the FSM operating range is not exceeded, the control architecture implements an offloading mechanism, which translates the FSM actuation commands to CPA reference angles. Effectively, this controller ensures that the FSM actuation will keep the mirror around its center position. Finally, it is worth noting that the controllers contain multiple transformation matrices to ensure that the associated quantities are expressed in the right coordinate frames.

### B. *Fibre coupling efficiency*

As highlighted in the design section of this paper, fibre coupling efficiency plays a critical role in the link budget of the LCT. To assess and optimize this efficiency, we utilize the FSM/ATS control loop to perform a circular tip/tilt scan with

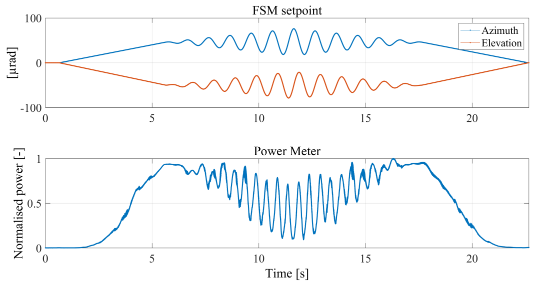


Fig. 9. The tip/tilt setpoints for the FSM/ATS control loop to perform a spiral scan, while simultaneously measuring the power coupled into the receive fibre

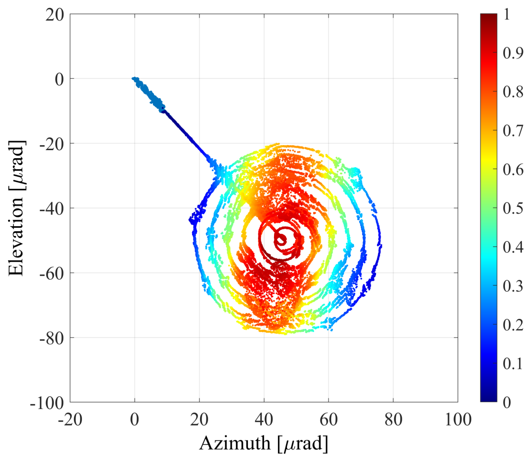


Fig. 10. The beam tip/tilt angles as measured by the ATS while performing a spiral scan around the expected receive fibre position, overlaid with colour to indicate the measured fibre signal power level

a radius of 30 µrad around the expected receive fibre position. During this scan, the energy coupled into the fibre is measured.

The results of this scan, depicted in Fig. 9 and 10, reveal an elongated spot shape. We attribute this shape to an optical aberration that we believe can be rectified through realignment of the optical bench. In ray tracing simulations, we observe that the oval spot shape leads to a fibre coupling efficiency of 36%, deviating from the theoretical coupling efficiency of a Gaussian beam. Empirical measurements confirm a ˜40% fibre coupling efficiency, consistent with the anticipated aberration-limited theoretical efficiency.

It's worth noting that the theoretical maximum fibre coupling efficiency in-flight is expected to be approximately 80% (-1 dB), as the terminal will receive a top-hat beam in the far field. We anticipate approaching this efficiency with the final setup and have allocated a loss margin of -1.7 dB to account for all static contributors.

We anticipate that dynamic wavefront errors resulting from atmospheric propagation, including tip/tilt errors, can be disregarded due to our operations in the stratosphere and the small 40 mm diameter aperture size.

However, there is a risk of fibre coupling loss due to local turbulence generated by minor thermal gradients within the Zephyr nose pod. Even in controlled lab conditions with a

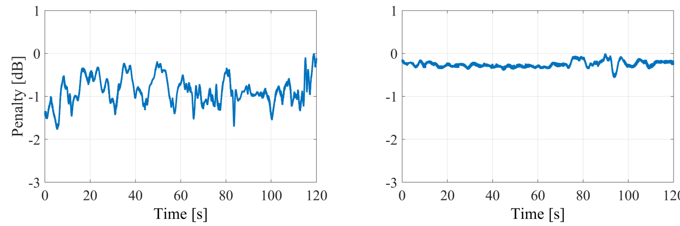


Fig. 11. Variance in fibre coupling efficiency due to turbulence in lab conditions (right figure is with the free space beam encapsulated in a tightly-fitting tube)

1 m free space link, we observed fibre coupling losses of up to -2 dB attributable to these small thermal gradients. By encapsulating the free space beam to mitigate thermal gradient effects, dynamic errors were limited to a loss of up to -0.5 dB. See Fig. 11.

We anticipate that the impact of thermal gradients on fibre coupling efficiency will scale with air pressure and become less significant in the stratosphere. The primary contributor to fibre coupling loss is expected to be tip/tilt tracking errors resulting from residual platform micro-vibrations. We have conducted FEM modelling and dynamic error budgeting to address this impact in the fibre coupling loss budget.

### *C. 1 Gbit/s Communications link*

Free space laser communication tests were conducted at various optical power levels to verify the optical signal-to-noise ratios and the achievable bit-error-rate (BER). A maximum BER of 1e-9 at a data throughput of 1 Gbit/s is targeted at an optical power level of -47.5 dBm.

Before performing the free space tests, the Laser Module provided by G&H is initially tested in a fibre-based loopback configuration. In this setup, the extinction ratio (ER) of the Laser Module output was measured at 10.5 dB. In this test, the modulator was provided with a random On-Off Keying (OOK) modulation signal at 1 GHz, amplified to an average output power of 1.2 Watts. The signal was then attenuated to a nominal optical power level of approximately -47.5 dBm before being fed back into the Rx path of the Laser Module. Within the Rx path, the signal was pre-amplified and detected by a balanced photodiode. This configuration yielded a Q-factor of greater than 10. The eye-diagram measurement is shown in Fig. 12.

In the final configuration, the Optical Modem was integrated, and the Early Prototype setup was employed to establish the free space optical communications link. The modem was used in a loopback BER-test mode, transmitting and decoding a 1.25 Gbit/s pseudo-random bit sequence (PRBS) using a hard-decision receiver to verify the accurate reception of bits. Forward error coding (FEC) in the form of Reed-Solomon (255,239) was applied to enhance link robustness.

To assess BER at various receiver signal power levels, a variable optical attenuator (VOA) was placed between the receiving optical bench and the Laser Module. The VOA allowed for controlled adjustments to the signal power level in

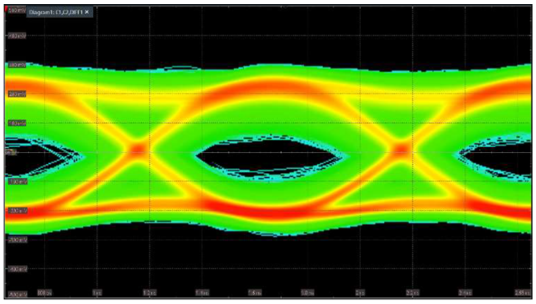

Fig. 12. Eye-diagram of a 1 GHz OOK-NRZ modulated signal after pre-amplification (-47.5 dBm input signal)

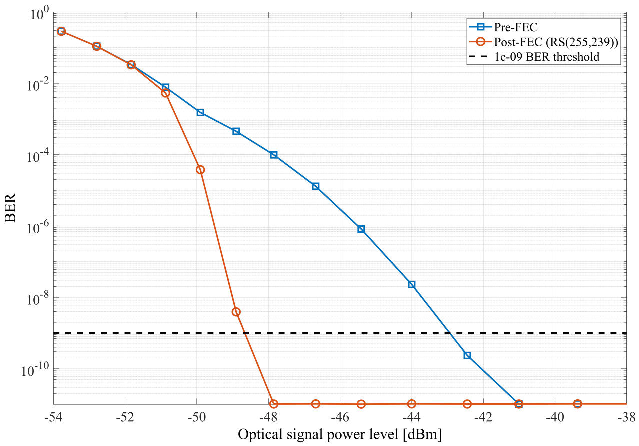


Fig. 13. Pre- and post-FEC bit error rates at various optical signal power levels, measured in the Early Prototype free space test setup

steps of approximately 2 dB while simultaneously recording the number of corrected and uncorrected bit errors over a 120-second interval. As depicted in Fig. 13, BER measurements were conducted both with and without FEC.

According to the link budget in Table I, the expected effective irradiance at the receiver is -37.3 dBm. At these power levels, as shown in Fig. 13, there were no bit errors observed. At signal levels of -42 dBm, bit errors occurred and were corrected by Reed-Solomon (RS) coding. Without RS coding, the 1e-9 BER threshold was exceeded at -43 dBm. A coding gain of approximately 5-6 dB was realized with FEC. When RS coding was applied, the BER threshold was exceeded only at power levels below -48 dBm, aligning with the link budget. The photon sensitivity with FEC stood at approximately 90 photons per bit at the 1e-9 BER threshold. This sensitivity limitation is attributed to slightly higher noise levels from the dual-polarization optical pre-amplifier, a trade-off for supporting any polarization state, and the capability of the Laser Module hardware to accommodate modulation and detection bandwidths for 10 Gbit/s data streams. The results of the free space communication link tests affirm a robust >10 dB link budget margin for the 1 Gbit/s 100 km Zephyr demonstration scenario.

## IV. Conclusions and Roadmap to Flight Experiments

The Early Prototype lab tests have been performed in parallel to the Zephyr LCT design, which is currently being finalized. An FSM control bandwidth of >250 Hz is demonstrated, and the fiber coupling efficiency is verified. The Laser Module and Optical Modem achieve a BER of 1e-9 at optical power levels below -48 dBm, which is >10 dB better than the expected in-flight irradiance levels. Hence, the lab tests confirm the large-margin link budget and provide useful input to the design process. Two Flight Prototypes will be built and tested to evaluate their performance and verify their robustness under representative environmental conditions. These tests will include thermal testing at low pressure to verify the terminal's resilience in challenging environments.

Upon the successful completion of the verification and qualification program, we will proceed with inter-Zephyr flight trials. These trials may potentially lead to the extension of the nominal link distance of 100 km between Zephyr platforms and an increase in data transfer rates.

Looking ahead, other logical progressions is to create a network of inter-connected Zephyrs and to explore the possibility of upgrading the terminal's design to support interoperability with other platforms, including Low Earth Orbit (LEO) satellites. This expansion of capabilities could open new avenues for high-speed data communication and collaboration in future wireless connectivity ecosystems.

## References


[1] H. Taguma, T. Nagoya, et al., "Study of coverage expansion of NTN by using optical communication between HAPS", unpublished (SKY Perfect JSAT Corporation)

[2] F. Heine, G. Mühlnikel, et al., "LCT for the European data relay system: in orbit commissioning of the Alphasat and Sentinel 1A LCTs", Proc. SPIE 9354, Free-Space Laser Communication and Atmospheric Propagation XXVII, 93540G, 2015

[3] L. C. Andrews and R. L. Phillips, "Laser Beam Propagation Through Random Media", 2nd ed, Bellingham, Washington: SPIE Press, 2005

[4] D. Giggenbach and H. Henniger, "Fading-loss assessment in atmospheric free-space optical communication links with on-off keying," Optical Engineering 47(4), 046001, 2008.

[5] J. Edmunds, L. Henwood-Moroney, et al., "Miniaturized optical communications modules for space applications", International Conference on Space Optics, ICSO 2020, 2020

[6] S. Kuiper, W. Crowcombe, et al., "High-bandwidth and compact fine steering mirror development for laser communications", 17th European Space Mechanisms and Tribology Symposium, 2017

[7] G. Witvoet, S. Kuiper and S. Meskers, "Performance validation of high-bandwidth Fine Steering Mirror for optical communications", International Conference on Space Optics, ICSO 2018 Article 1118061, 2018